# Origin of Antiferroelectricity in $NH_4H_2PO_4$ from First Principles

J. Lasave,[1] S. Koval,[1,2,*] N. S. Dalal,[2] and R. L. Migoni[1]

[1]*Instituto de Física Rosario, Universidad Nacional de Rosario and CONICET, 27 de Febrero 210 Bis, 2000 Rosario, Argentina*
[2]*Department of Chemistry and NHMFL, Florida State University, Tallahassee, Florida 32306, USA*

(Received 5 March 2007; published 27 June 2007)

The low-temperature antiferroelectric (AFE) phase of $NH_4H_2PO_4$ corresponds to H ordering in O-H-O bridges leading to $H_2PO_4$ group polarizations perpendicular to the tetragonal $c$ axis and alternating in chains. We determine the microscopic origin of such order by means of first-principles calculations in the framework of the density functional theory. The formation of N-H $\cdots$ O bridges with correlated charge transfers and $NH_4^+$ group distortions turn out to be essential in stabilizing the AFE configuration against a $c$-polarized ferroelectric (FE) phase, as well as other FE states polarized perpendicular to the $c$ axis. These FE states lie only a few meV above the AFE phase, which explains the observation of FE-AFE phase coexistence near the AFE transition.

DOI: 10.1103/PhysRevLett.98.267601 PACS numbers: 77.84.Fa, 77.80.−e

$KH_2PO_4$ (KDP) and its isomorphs have been considered as prototype materials for understanding the cooperative mechanism of hydrogen-bonded systems, ever since the discovery of their ferroelectric properties in the late 1930's [1]. In spite of extensive efforts since then, the microscopic origin of their ferroelectric (FE) or antiferroelectric (AFE) behavior is still not fully understood [1–3]. For example, the mechanism behind the large effect of deuteration on the transition temperature is still being debated as to whether it is caused by pure tunneling (Blinc's model) [2] or bond geometry effects [3,4]. Recent *ab initio* calculations have shown that in fact both of the effects play synergistic roles [5]. Another long-standing issue is how the substitution of the $NH_4^+$ ion in place of $K^+$, results into antiferroelectricity; i.e., what causes $NH_4H_2PO_4$ (ADP) to be antiferroelectric ($T_c = 148$ K) [3].

As has been well established via neutron diffraction, the major difference between the structures of the ferroelectric KDP and antiferroelectric ADP is the positions of the acid hydrogens ($H_O$'s) in the O-H $\cdots$ O bonds. A schematic of the structural differences is shown in Fig. 1(a) for ADP and (b) for KDP as viewed along their tetragonal ($z$) axes. In both compounds, the $PO_4$ groups have only 2 H's attached to the O's, according to the so-called ice rules. In ADP, these two "close" H's are attached laterally so as to lead to the $[H_2PO_4]^-$ dipole pointing to the basal ($xy$) plane, while in KDP the corresponding dipole points along the $z$ direction [6]. Interestingly, this lateral H bonding for ADP was predicted by Nagamiya in 1952 [7], well before its verification by neutron diffraction [8]. Subsequently, however, Ishibashi *et al.* [9,10] showed that the basal plane can also lead to ferroelectric phases, and that the different phases probably have comparable energetics. They suggested empirically that some form of dipolar interactions must be introduced in order to stabilize the antiferroelectric phase. Some evidence for the coexistence of the FE and AFE domains has been seen in EPR studies on ADP using $(AsO_4)^{4-}$ radical as probe [11,12], but there has been no further theoretical justification. More recently, Schmidt has provided an insightful discussion of the role of $NH_4^+$ ion, based on the neutron diffraction data of Hewat [13], and proposed that perhaps an effective interaction between the $NH_4^+$ protons ($H_N$'s) and the $H_O$'s provides the needed dipolar coupling [3], but a quantitative explanation of the underlying mechanism for antiferroelectricity, and, in particular, of the closeness of the FE and AFE domain formation energies is still lacking.

In this Letter, we report results from first-principles calculations that clarify the following long-standing questions regarding ADP: (1) what is the microscopic origin of antiferroelectricity in ADP; (2) what is the role of $NH_4^+$ ions and the N-H $\cdots$ O bonds in favoring the AFE states; and (3) how close in energy are the AFE and FE states, actually? The results provide a clear microscopic mechanism of antiferroelectricity in ADP and related ammonium-based materials.

The DFT calculations have been carried out using the SIESTA code [14,15]. This method employs a linear combination of pseudoatomic orbitals (LCAO) of the Sankey-

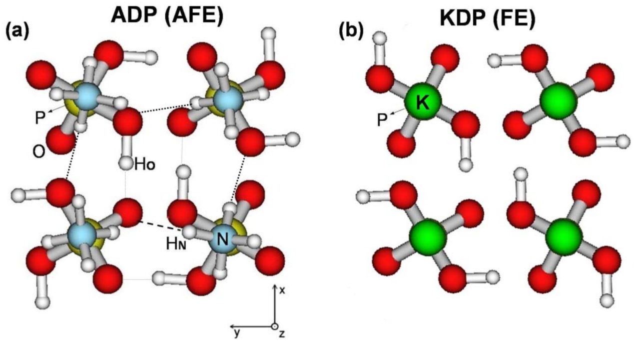

FIG. 1 (color online). Schematic representation of (a) ADP (AFE) and (b) KDP (FE) structures from a top ($z$ axis) view. In the ADP case, short and long N-H $\cdots$ O bonds are indicated by long-dashed and dotted lines, respectively.

Niklewsky type as basis functions [16]. For the representation of the valence electrons we used double-zeta bases with polarization functions (DZP) and an orbital confinement energy of 50 meV. The exchange-correlation energy terms were computed using the Perdew-Burke-Ernzerhof (PBE) form of the generalized gradient approximation [17]. We used nonlocal, norm-conserving Troullier-Martins pseudopotentials [18] to eliminate the core electrons from the description. Further details can be found in our earlier work related to KDP [5,6,19].

The paraelectric (PE) phase of ADP has a body-centered tetragonal (bct) structure with 2 f.u. per lattice site (24 atoms). However, for the different phases (FE, AFE, and PE) we used the equivalent conventional face-centered tetragonal (fct) cell (containing 8 f.u.). With this large supercell, the Brillouin zone Γ point alone provides a sufficient sampling in the calculations performed.

We start from the PE experimental structure of ADP at 152 K, with the hydrogens fixed at the average positions in the O-H-O bond centers. The full-atom relaxation with the above constraint for the acid $H_O$ to mantain the PE phase, leads to an O-O distance underestimated by $\approx 0.04$ Å compared to the experiment [20]. This is in part due to the constraint, but also to the approximate character of the exchange-correlation term, as we also found in similar calculations for KDP [5]. To avoid effects of this feature, we fix the O positions to the experimental values, and relax all the remaining atoms. The resulting structural parameters for the calculated PE phase compare very well with the available experimental data [21].

We perform different calculations to study the AFE and FE instabilities and their relative importance in ADP. We first consider the joint displacement of N and the acid $H_O$ protons, notated as $u_N$ and $u_{H_O}$, respectively, as they move away from their centered positions in the PE phase of ADP in two cases: (1) following the AFE pattern of distortion [see Fig. 2(c)], and (2) following the FE pattern [see Fig. 2(b)]. In these and all the following calculations the $H_N$'s of the ammonium and P's are allowed to relax unless we state the contrary, while the O's remain fixed for the reasons underlined above. In Fig. 2(a) we plot with squares symbols the *ab initio* total-energy curve as a function of $u_{H_O}$, for the concerted motion of $H_O$ and N corresponding to each pattern. The calculated minimum-energy AFE state has a structure in fairly good agreement with the available x-ray data [20], and, as expected, is more stable than the FE counterpart, but their energy difference is only 3.6 meV/f.u. as shown in Fig. 2(a). If the O atoms are further allowed to relax, the AFE state remains 1.25 meV/f.u. below the FE one. This difference grows to $\approx$3.8 meV/f.u. with additional relaxations of the lattice parameters according to the symmetries of each phase. Thus, our calculations confirm that the FE state is indeed very close in energy above the AFE one in ADP, supporting the Ishibashi's model [9,10], and also providing a rationalization of the earlier evidence of FE and AFE regions near the AFE transition [11,12].

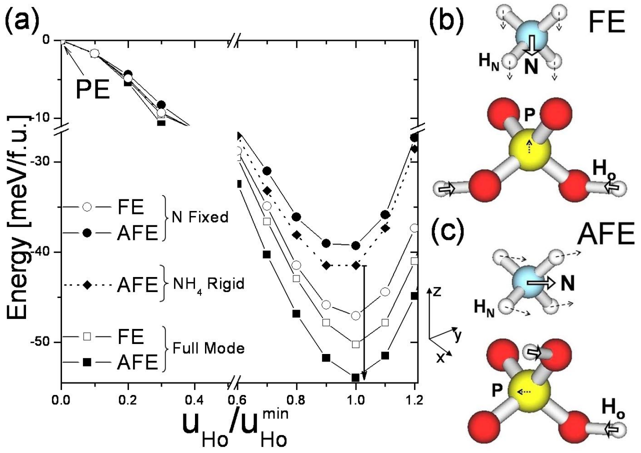

FIG. 2 (color online). (a) Energy as a function of the acid H displacement $u_{H_O}$ for different patterns of atomic displacements corresponding to the FE and AFE distortions depicted in Figs. 2(b) and 2(c), respectively. $u_{H_O}^{min}$ denotes the $H_O$ displacement at the corresponding energy minimum. In addition to the full FE or AFE modes, other curves show the effect of imposing different constraints while performing the FE or AFE modes: N fixed or $NH_4^+$ moved rigid as in the PE phase. Lateral views of the ADP formula unit indicate the atomic displacements in the FE (b) and AFE (c) modes. White arrows correspond to displacements imposed according to each mode, dashed arrows to concomitant relaxations.

In the calculated AFE state, the $NH_4^+$ ion displaces laterally in the *xy* plane by $u_N^{min} = 0.09$ Å [see Fig. 2(c)] and produces a dipole, which reinforces the one determined by the lateral arrangement of acid protons in the phosphate. This is in contrast to the calculated FE phase, where the $NH_4^+$ ions displace along the *z* direction about 0.05 Å [see Fig. 2(b)] reinforcing the *z* dipoles produced by the arrangement of acid protons in the phosphates, analogous to the behavior of K in KDP [see Fig. 1(b)].

To look now for the mechanism for the stabilization of the AFE vs FE state, we analyze the energy contribution of the N and $H_O$ motion separately. By setting $u_{H_O} = 0$ we observe that a finite displacement $u_N$ along *z* for the ammonium [see Fig. 2(b)] does not contribute to any energy instability in the FE case, and its displacement along the *xy* plane in the AFE case [see Fig. 2(c)] produce a very tiny instability (less than 1 meV/f.u.). Alternatively, we move the acid $H_O$'s and set $u_N = 0$; i.e., N's are fixed to their positions in the PE phase [see Figs. 2(b) and 2(c)]. In this case, a larger energy decrease is observed for the FE pattern compared to the AFE one [see circles in Fig. 2(a)]. Here, the $H_N$'s relaxations in the $NH_4^+$ groups are very small in contrast with the case where N and $H_O$'s are both allowed to move. The inclusion of the N motion together with the $H_O$'s displacements in the FE case leads to a further energy decrease of less than 10% from the total instability [see open circles and squares at the energy minima in Fig. 2(a)]. Since, as already mentioned, the relaxation with $u_{\mathrm{H_O}} = 0$ does not produce any instability, we conclude that the source of the FE instability in ADP is the acid proton off-centering ($u_{\mathrm{H_O}} \neq 0$), similar to what is found in KDP [5]. The AFE instability is also mainly driven by the proton off-centering, however this motion alone is insufficient to produce antiferroelectricity in ADP.

Finally, we move all atoms according to the pattern of the AFE mode, except that the structure of the $\mathrm{NH_4^+}$ groups is kept symmetric as in the PE phase and rigid. The energy decrease, shown by the solid diamonds in Fig. 2(a), is to be compared with the one shown by the open squares, corresponding to the fully relaxed FE phase, because in this case the $\mathrm{H_N}$ relaxations in the $\mathrm{NH_4^+}$ groups are negligible. We conclude that as long as the $\mathrm{NH_4^+}$ tetrahedra are not allowed to deform by relaxing their $\mathrm{H_N}$'s, the FE state is more stable than the AFE one. Only such $\mathrm{NH_4^+}$ relaxations, which allow the optimization of N-H $\cdots$ O bridges, produce the energy decrease shown by the arrow between full diamonds and squares at $u_{\mathrm{H_O}}/u_{\mathrm{H_O}}^{\mathrm{min}} = 1$ in Fig. 2(a). Therefore, the stabilization of the AFE state against the FE one has to be ascribed to the optimal formation of N-H $\cdots$ O bridges.

The role of the N-H $\cdots$ O bonds in the stabilization of the AFE state was further supported by the energy variation produced by a global rigid rotation of angle $\theta$ of the $\mathrm{NH_4}^+$ molecules around the $z$ axis, starting from the minimum-energy configurations for the AFE and FE states where $\theta$ is set to zero. We assume that the main effect of these rotations is the rupture of the N-H $\cdots$ O bonds. We observe that the energy increases in similar amounts in both phases, therefore to make more evident the differences we refer the energies to the ones corresponding to equal rotations in the PE phase. The resulting curves are plotted in Fig. 3. We observe that for a rotation angle larger than $\approx 20°$, the FE phase becomes more stable than the AFE one. This is a further verification of the importance of the N-H $\cdots$ O bridges in stabilizing the AFE phase.

For each O-H $\cdots$ O bond, one oxygen participates in a short N-H $\cdots$ O bond while the other participates in a long N-H $\cdots$ O bond. The acid $\mathrm{H_O}$ proton is closer to the oxygen of the long N-H $\cdots$ O bond [see Fig. 1(a)]. The existence of these two types of bonds has been suggested earlier [3]. We analyze the charge redistributions in both types of N-H $\cdots$ O bonds produced in the full AFE mode in going from the PE state ($u_{\mathrm{H_O}} = 0$) to the AFE minimum at $u_{\mathrm{H_O}}/u_{\mathrm{H_O}}^{\mathrm{min}} = 1$ [see solid squares in Fig. 2(a)]. The charge density difference $\rho^{\mathrm{AFE}}(r) - \rho^{\mathrm{PE}}(r)$ is plotted on the planes defined by the acid H bond and the N of the short [Fig. 4(a)] and long [Fig. 4(b)] N-H $\cdots$ O bonds. Besides the charge redistribution in the acid $\mathrm{H_O}$ bond, which is similar to that found in KDP [5,19], we observe a depletion of charge along the long N-H $\cdots$ O bond [see top of Fig. 4(b)] and a noticeable charge increase along the short N-H $\cdots$ O bond [see top of Fig. 4(a)]. The net result is a charge flow from the N-H $\cdots$ O bond which becomes longer to the one which shortens in the AFE state, producing a distortion of the $\mathrm{NH_4^+}$ molecules, as experimentally observed [20].

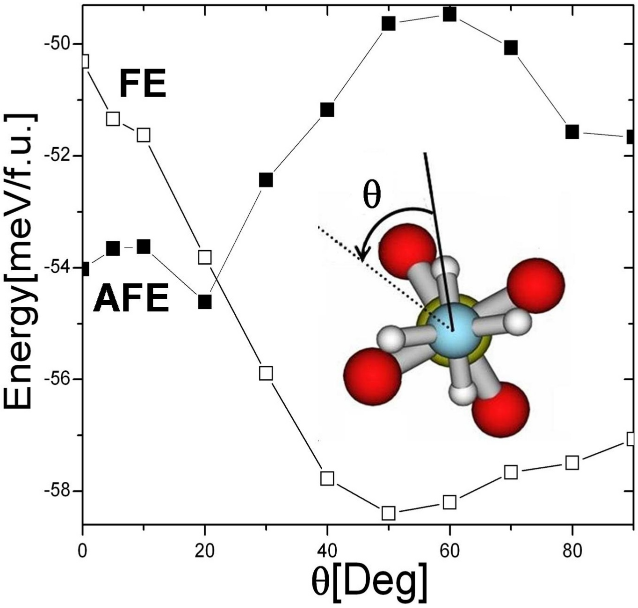

FIG. 3 (color online). *Ab initio* energy of the AFE (solid squares) and the FE (open squares) phases relative to the PE phase, as a function of the rotation angle $\theta$ of the $\mathrm{NH_4^+}$ ion, as explained in text. $\theta = 0$ is the ammonium angular position corresponding to the minimum-energy relaxed states.

We analyzed the charge redistributions in the same bond systems occurring in the case of full FE distortions [see bottom of Fig. 4(a) and 4(b)]. The charge density difference $\rho^{\mathrm{FE}}(r) - \rho^{\mathrm{PE}}(r)$ is fairly similar to the AFE case in the acid H bond, while almost no charge redistributions are obseved in the N-H $\cdots$ O bonds. In this case, almost no charge transfer occurs in the N-H $\cdots$ O bonds, in part because the ammonium ion does not displace, for symmetry reasons, along the $xy$ plane relative to the P atom. In fact the $\mathrm{NH_4}^+$ displacement along the $z$ direction does not lead to differentiated short and long N-H $\cdots$ O bonds with their neighboring oxygens.

We also studied the relative stability of two other possible ordered phases with translational symmetry and $xy$-polarized $\mathrm{PO_4}$ tetrahedra, as proposed by Ishibashi *et al.* [9]: an hypothetical $\mathrm{FE_1}$ phase with $C_s^4$ symmetry and a $\mathrm{FE_2}$ phase sketched in Fig. (1d) of Ref. [9], where FE ordered $\mathrm{PO_4}$-chains alternate with perpendicularly polarized AFE ordered $\mathrm{PO_4}$-chains. In Fig. 4(c) we show the energy differences of these states and the $z$-polarized FE one depicted in Fig. 2(b) relative to the AFE minimum calculated with the experimental lattice parameters of the PE phase. $\mathrm{FE_1}$ and $\mathrm{FE_2}$ phases lie very close above the AFE phase ($\approx 5$ and 11 meV/f.u., respectively) in agreement with Ishibashi's prediction. These differences should grow

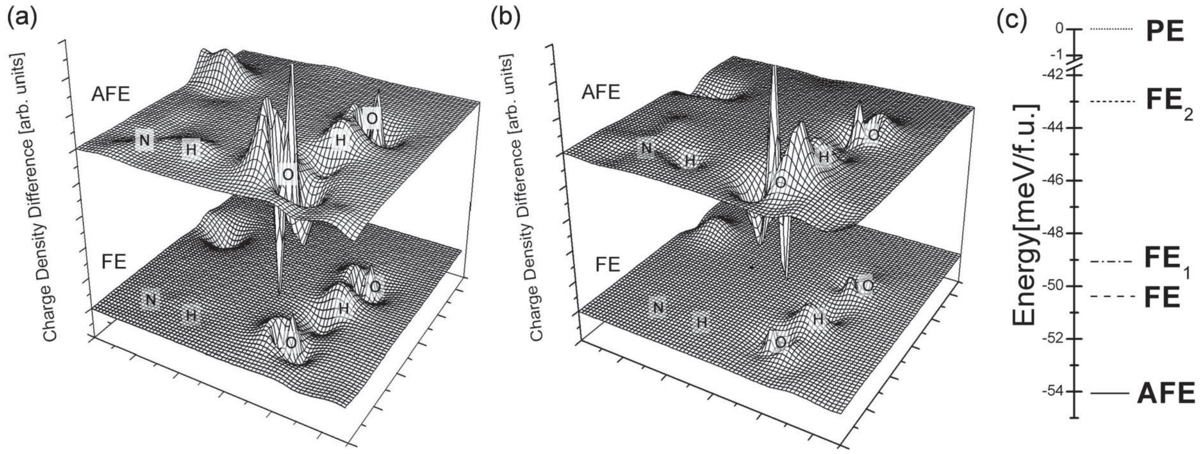

FIG. 4. (a) Charge density differences $\rho^{\mathrm{AFE}}(r) - \rho^{\mathrm{PE}}(r)$ (top) and $\rho^{\mathrm{FE}}(r) - \rho^{\mathrm{PE}}(r)$ (bottom) in the plane defined by the acid H bond and the short N-H $\cdots$ O bond of ADP. (b) Same as (a), but in the plane defined by the acid H bond and the long N-H $\cdots$ O bond [see Fig. 1(a)]. (c) *Ab initio* energy levels of the PE, *xy*-polarized ferroelectric (FE$_1$ and FE$_2$), *z*-polarized FE, and AFE states in ADP (see explanations in text).

with relaxation of the lattice parameters, as for the *z*-polarized FE state.

Summarizing, this work elucidates the microscopic mechanism of how antiferroelectricity arises in ADP (and its isomorphs such as $NH_4H_2AsO_4$, and their deuterated analogs) using first-principles electronic structure calculations. The data clearly show that the AFE phase of ADP is only a few meV below its possible FE phases, which is consistent with the observation of the FE phase coexistence near the AFE transition [11,12]. The energy imbalance in favor of the AFE phase is provided by the strengthening of N-H $\cdots$ O bonds, which distort the $NH_4^+$ ion, repel the acid H that is close to the stronger N-H $\cdots$ O bond, involve significant charge transfers, and thus create dipole moments in the plane of the O-H $\cdots$ O bonds, in full agreement with the neutron data [13] and Schmidt's conjecture [3]. Further computational developments using *ab initio* techniques should enable us to estimate the contribution of such sought-after, finer effects as the role of deuteration of the N-H hydrogens vs O-H hydrogens, which has not yet been possible experimentally.

This work was supported partially with Grant No. PICT 03-14599 of ANPCyT, Argentina. We thank V. H. Schmidt, R. Blinc, A. Bussmann-Holder and O. Gunaydin-Sen for very helpful discussions.

---

*Corresponding author.
koval@ifir.edu.ar

[1] R. Blinc, Ferroelectrics **301**, 3 (2004).
[2] R. Blinc and B. Zeks, Ferroelectrics **72**, 193 (1987).
[3] V. H. Schmidt, Ferroelectrics **72**, 157 (1987).
[4] M. I. McMahon *et al.*, Nature (London) **348**, 317 (1990).
[5] S. Koval, J. Kohanoff, R. L. Migoni, and E. Tossati, Phys. Rev. Lett. **89**, 187602 (2002); S. Koval, J. Kohanoff, J. Lasave, G. Colizzi, and R. L. Migoni, Phys. Rev. B **71**, 184102 (2005).
[6] J. Lasave, S. Koval, N. S. Dalal, and R. Migoni, Phys. Rev. B **72**, 104104 (2005).
[7] T. Nagamiya, Prog. Theor. Phys. **7**, 275 (1952).
[8] L. Tenzer, B. C. Frazer, and R. Pepinsky, Acta Crystallogr. **11**, 505 (1958).
[9] Y. Ishibashi, S. Ohya, and Y. Takagi, J. Phys. Soc. Jpn. **33**, 1545 (1972).
[10] Y. Ishibashi, S. Ohya, and Y. Takagi, J. Phys. Soc. Jpn. **37**, 1035 (1974).
[11] B. Lamotte, J. Gaillard, and O. Constantinescu, J. Chem. Phys. **57**, 3319 (1972).
[12] N. S. Dalal, J. A. Hebden, D. E. Kennedy, and C. A. McDowell, J. Chem. Phys. **66**, 4425 (1977).
[13] A. W. Hewat, Nature (London) **246**, 90 (1973).
[14] P. Ordejón, E. Artacho, and J. M. Soler, Phys. Rev. B **53**, R10 441 (1996).
[15] D. Sánchez-Portal, P. Ordejón, E. Artacho, and J. M. Soler, Int. J. Quantum Chem. **65**, 453 (1997).
[16] O. F. Sankey and D. J. Niklewsky, Phys. Rev. B **40**, 3979 (1989).
[17] J. P. Perdew, K. Burke, and M. Ernzerhof, Phys. Rev. Lett. **77**, 3865 (1996).
[18] N. Troullier and J. L. Martins, Phys. Rev. B **43**, 1993 (1991).
[19] S. Koval, J. Kohanoff, R. L. Migoni, and A. Bussmann-Holder, Comput. Mater. Sci. **22**, 87 (2001).
[20] T. Fukami, S. Akahoshi, K. Hukuda, and T. Yagi, J. Phys. Soc. Jpn. **56**, 2223 (1987).
[21] N. Pérès, M. Souhassou, B. Wyncke, G. Gavoille, A. Cousson, and W. Paulus, J. Phys. Condens. Matter **9**, 6555 (1997).